Observation of magnetization saturation of $CuGeO_3$ in ultrahigh magnetic fields up to 500 T

H. Nojiri, Y. Shimamoto, and N. Miura
Institute for Solid State Physics, University of Tokyo, 7-22-1 Roppongi, Tokyo 106, Japan

M. Hase and K. Uchinokura
Department of Applied Physics, University of Tokyo, 7-3-1 Hongo, Tokyo 113, Japan

H. Kojima, I. Tanaka, and Y. Shibuya
Institute of Inorganic Synthesis, Yamanashi University, Kofu-shi, Yamanashi 400, Japan
(Received 13 March 1995)

The magnetization in a spin-Peierls material $CuGeO_3$ was measured by means of the Faraday rotation in ultrahigh magnetic fields up to 500 T. The experimental magnetization curve shows a nonlinear increase against the magnetic field which is a typical behavior of a one-dimensional quantum spin system. A distinct saturation of the magnetization was observed at 253 T, from which the exchange parameter is evaluated as 183 K. A large hysteresis of the magnetization was observed in the magnetic phase, whereas it was indiscernible in the uniform phase.

I. INTRODUCTION

Low-dimensional quantum spin systems have attracted much attention in these decades both theoretically and experimentally. Various new magnetic materials based on Cu oxides have been recently investigated as model materials. There are many interesting and unsolved problems in these low-dimensional quantum spin systems regarding either Haldane's conjecture or the spin-Peierls transition. $CuGeO_3$ is one of these materials, and was discovered by Hase, Terasaki and Uchinokura.[1] It attracts much attention as an inorganic material which shows the spin-Peierls transition. The spin-Peierls transition has been investigated for more than a decade in several model materials, but only for organic substances. Extensive studies on organic systems have solved many of the fundamental problems concerning the mechanism of the spin-Peierls transition. However, due to the complicated structures and the difficulties in preparing large single crystals of the organic compounds, several unsolved problems remain, such as understanding the nature of the field-induced magnetic phase.

Since the discovery the $CuGeO_3$, many experimental results have been reported on this new material, but there have been large discrepancies among the estimated values of the exchange constant J, which is the most important parameter in this system. Throughout this paper, we define J by the following Hamiltonian of the spin system:

$$H = J\sum_{ij} \mathbf{S}_i \cdot \mathbf{S}_j . \tag{1}$$

Hase, Terasaki, and Uchinokura[1] have shown that the temperature dependence of the magnetic susceptibility has a large deviation from the theoretical curve by Bonner and Fisher[2] for an $S=\frac{1}{2}$ one-dimensional Heisenberg antiferromagnet. They estimated the value of $J=88$ K from the peak of the magnetic susceptibilities.

Nishi, Fujita, and Akimitsu[3] made an inelastic neutron scattering experiment, and obtained a value of $J=120.4$ K by applying the des Cloizeaux-Pearson formula[4] for the dispersion of the magnetic excitations. However, it is not clear that the des Cloizeaux-Pearson formula is applicable for spin-Peierls systems which have a completely different ground state from normal antiferromagnets. Therefore, the most direct method to determine the exchange constant of an antiferromagnet is to measure the magnetization and its saturation. In the case of $CuGeO_3$, we need a magnetic field of several hundreds of T to observe a full magnetization curve. The recent advance of the electromagnetic flux compression technique has enabled us to perform such a measurement up to 500 T. This measurement also gives us a crucial clue whether $CuGeO_3$ can be considered as a simple quasi-one-dimensional chain through a comparison with the theoretical curve by Griffiths[5] or Bonner and Fisher.[2]

A study of the full magnetization curve above the saturation field will provide interesting information about the nature of the magnetic phase of spin-Peierls materials. Hase *et al.*[6] determined the magnetic phase diagram of $CuGeO_3$ in magnetic fields up to 25 T by means of magnetization measurements and showed that there is a universality in the magnetic phase diagram among $CuGeO_3$ and organic spin-Peierls materials by scaling the temperature and magnetic field axes. A schematic phase diagram for a spin-Peierls system on a magnetic field-temperature plane is shown in Fig. 1. D, U, and M denote the dimerized, uniform, and magnetic phases, respectively. In the uniform phase, the system can be considered to be a uniform linear chain Heisenberg antiferromagnet. Below the spin-Peierls transition temperature T_{sP}, spins are in the dimerized phase where they are in a nonmagnetic singlet state with the dimerization of the lattice. When a magnetic field is applied to the system at a temperature below T_{sP}, it shows a nonlinear increase of the magnetization at H_c. Below T_{Tc}, the transition between the dimerized phase and magnetic phase is of the first order and is accompanied by hysteresis. The nature of the field-induced

0163-1829/95/52(17)/12749(6)/$06.00

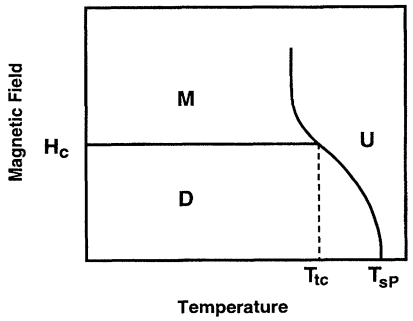

FIG. 1. Schematic phase diagram for a spin-Peierls system. D, U, and M denote dimerized, uniform, and magnetic phase, respectively. T_{sP} is the spin-Peierls transition temperature and H_c is the critical field from the dimerized phase to the magnetic phase. The hysteresis of magnetization observed at H_c below $T=T_{T_c}$.

magnetic phase has been intensively studied since the discovery of the spin-Peierls transition, and is considered to be either a new commensurate phase, a magnetic soliton, or an incommensurate phase. U, D, and M phases meet together at a point $[T_{T_c}, H_c(T_{T_c})]$ but the details of the phase diagram around this point and the precise temperature dependence of H_c are not yet so clear.

In this paper, we present the results of the Faraday rotation experiments up to 500 T. The value of the exchange constant and the magnetic properties of $CuGeO_3$ in ultrahigh magnetic fields will be discussed.

II. EXPERIMENTAL

In magnetic fields higher than 100 T (MG fields), ordinary magnetization measurements using inductive pickup coils are impossible because of large induction voltages. The induction voltage is proportional to the time derivative of the magnetic flux. In the case of MG fields, a typical rise time of the field is much shorter than that for nondestructive pulsed fields up to about 50 T, and hence the induction voltage is about 1000 times larger. Therefore, we performed measurements of the magnetization by means of the Faraday rotation, which is not affected by the large induction voltages.

We used two different techniques to generate the high magnetic fields. The first one is the single turn coil technique.[7] Figure 2 shows the trace of a magnetic field produced by the single turn coil technique. Magnetic fields up to 150 T are available with a bore of 10 mm. The sample temperature can be lowered down to liquid He temperatures. The shape of the pulsed field is sinusoidal with a half period of about 6 μs. In this type of field, hysteresis in the magnetization process can be measured. After every shot, the coil is destroyed, but the sample set at the center of the coil remains unbroken because the coil blows up towards the outer direction. To generate magnetic fields higher than 150 T, the second technique, electromagnetic flux compression, is employed.[8,9] It is a method which compresses the magnetic flux by an imploding metal ring called the liner. The initial magnetic flux of 2–3 T is magnified more than 200 times in this process. Magnetic fields as high as 500 T with a bore of about 10 mm are available by this method. The sample temperature can be controlled also in this case down to liquid He temperatures. Figure 3 shows a trace of the magnetic field in the electromagnetic flux compression. The magnetic field first rises exponentially and after that it shows an almost linear increase against time above around 300 T. Although the sample and cryostat are broken at every shot, we can repeat experiments with an interval of approximately 1 or 2 days.

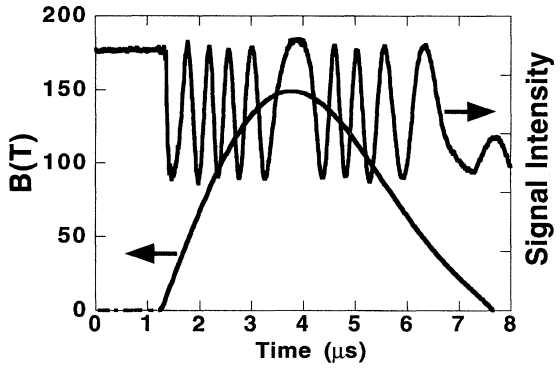

FIG. 2. Example data of the Faraday rotation signal and magnetic-field trace obtained by using single turn coil technique. The sample thickness is 0.5 mm. The wavelength is 514.5 nm.

The Faraday rotation angle is composed of both magnetic and nonmagnetic parts. As is well known, the magnetic part of the Faraday rotation is expressed in the odd power series of the magnetization. Namely, the rotation angle θ is expressed as follows:

$$\theta=\theta_0(H)+A_1M+A_3M^3+A_5M^5+\cdots, \qquad (2)$$

where $\theta_0(H)$ is a nonmagnetic part, M is the magnetization, and $A_1, A_3, \ldots$ are coefficients. In practice, the nonmagnetic contribution $\theta_0(H)$ in $CuGeO_3$ is very small and can be neglected, as will be shown in the next section. In low magnetic fields, the rotation angle is almost linear with respect to the magnetization. In the higher field range, contributions of higher order terms, the third and fourth terms in (2), should be considered. The microscopic origin of the magnetic Faraday rotation is the spin-orbit splitting of the excited states. It

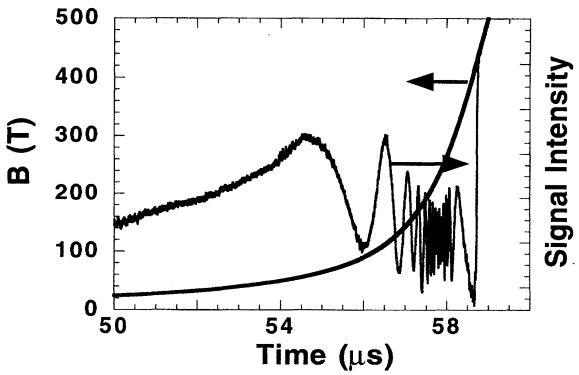

FIG. 3. Plot of a magnetic field and a Faraday rotation signal vs time in electromagnetic flux compression experiment. The sample thickness is 0.27 mm. The wavelength is 514.5 nm.

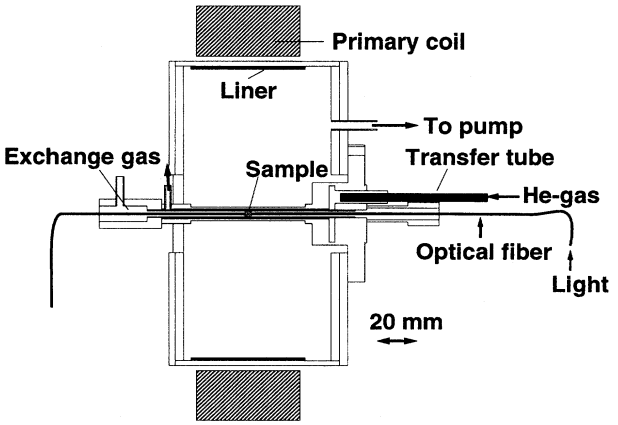

FIG. 4. Experimental setup for electromagnetic flux compression experiment.

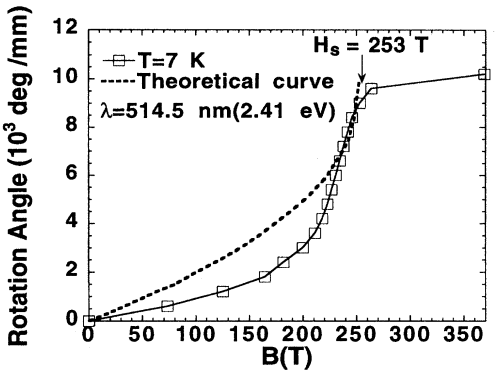

FIG. 5. Plot of the Faraday rotation angle against the magnetic field. The wavelength is 514.5 nm from an Ar laser. The data points correspond to the extrema of the Faraday rotation signal. The solid line is the guide for eyes. Dashed line is the theoretical curve for an $S=\frac{1}{2}$ uniform Heisenberg antiferromagnetic chain at $T=0$ K from Refs. 2 and 5.

makes a difference in transition probabilities between right and left circularly polarized lights in the transition from the ground $d\gamma$ orbit to excited $d\varepsilon$ orbits. When the photon energy of the incident light is close to the energy of the $d\gamma$-$d\varepsilon$ gap, the contribution of the higher order terms to the Faraday rotation cannot be neglected and the rotation angle is nonlinear to the magnetization. The nonlinearity can be neglected when the photon energy of the incident light is considerably smaller than this transition energy. Therefore, it is necessary to perform Faraday rotation measurements in different photon energies to derive a true magnetization curve from the Faraday rotation data.

Terasaki *et al.*[10] reported on the optical reflection measurements for $CuGeO_3$. According to their results, there is an absorption band due to the charge transfer between Cu and oxygen at around 1.25 eV. The origin of another absorption around 2.4–2.8 eV is considered to be the $d\gamma$-dε transition. The absorption for the charge transfer explains the blue color of $CuGeO_3$. The present results of optical transmission measurements give a result consistent with their data. In the present work, we performed the Faraday rotation measurements in two different photon energies, 2.41 eV (514.5 nm) from an Ar laser and 1.08 eV (1152 nm) from a near-infrared He-Ne laser. The former photon energy is close to the $d\gamma$-$d\varepsilon$ transition energy and a nonlinearity is expected in Faraday rotation. In fact, we observed the nonlinearity at 2.41 eV when we compared the Faraday rotation with the magnetization in the lower field range up to 40 T. Contrary to this, the nonlinearity in the near-infrared range 1.08 eV was found to be negligibly small.

Figure 4 shows the experimental setup for the electromagnetic flux compression experiment. Optical fiber cables are used for the light transmission. The sample is sandwiched between two Polaroid linear polarizing sheets. The transmitted light is sent to an avalanche photodiode detector located in a shield room through an optical fiber cable. The use of an optical fiber is very useful to reduce a noise generated at the start of current discharge in the field production. The magnetic field is measured by using a pickup coil. The error in the measurement of the magnetic field intensity is about 1%. The optical and magnetic-field signals are digitized and stored in transient recorders and then analyzed by a computer. Low temperatures down to liquid He temperatures can be obtained by a He gas flow-type cryostat. It is made of a special kind of fiber reinforced plastic which is leak tight even at low temperatures. The liner is located inside the vacuum chamber to avoid the generation of shock waves. Figures 2 and 3 show traces of the Faraday rotation. From such traces, the rotation angle was obtained by an arcsine transformation.

Single crystal samples were grown by the floating-zone method, and they were cut along their a faces by cleaving. The magnetic field was applied parallel to the a axis. The polarized axis of the incident light was set to 45° from the b and c axes. $CuGeO_3$ shows a dichroism, especially at 514.5 nm.

III. RESULTS

The magnetic-field dependence of the Faraday rotation angle at 514.5 nm is shown in Fig. 5. The rotation angle shows a distinct saturation at around 250 T. There is no heating of the sample during the field production by eddy current because both the sample and the cryostat are insulators. The effect of the adiabatic heating which should be considered in a paramagnetic phase can be neglected because the present measurements were made in an ordered phase. Bonner *et al.*[11] calculated the magnetization curve for an alternating Heisenberg antiferromagnetic chain. Their result shows that the magnetization curve of alternating systems becomes very close to that of a uniform system in high magnetic fields near the saturation field. Although the spin-Peierls state is not exactly the same as the alternating system, this fact implies that it would be meaningful to compare the present results in high fields with the theoretical curve[2] for an $S=\frac{1}{2}$ uniform Heisenberg antiferromagnetic chain at $T=0$ K as plotted in Fig. 5 for comparison. The experimental data show a large deviation from the theoretical curve. The discrepancy is due to the contribution of the higher order terms in the Faraday rotation, because the photon energy, 2.41 eV, of the incident light is close to the $d\gamma$-$d\varepsilon$ transition energy, as discussed in Sec. II. In this case, the contribution of these

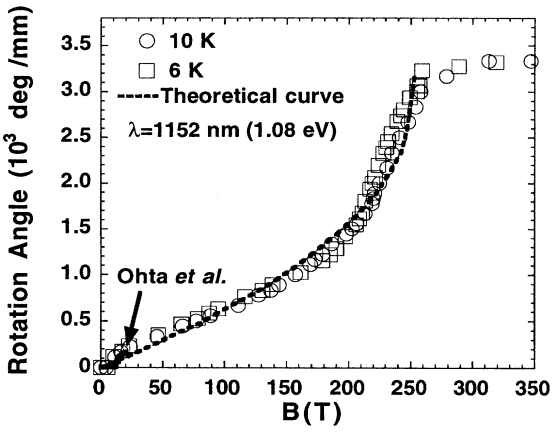

FIG. 6. Plot of the Faraday rotation angle against the magnetic field. The wavelength is 1152 nm from a He-Ne laser. Dashed line is the theoretical curve for an $S=\frac{1}{2}$ uniform Heisenberg antiferromagnetic chain at $T=0$ K from Refs. 2 and 5. Thick line shows the magnetization data from Ref. 12.

higher order terms is almost of comparable order with that of the linear term. In spite of this nonlinearity in the Faraday rotation, the saturation field can be determined from the saturation of the rotation angle, because the nonlinearity does not affect the kink at saturation. The very small increase of the rotation angle above the saturation field may be due to the Van Vleck paramagnetism.

Figure 6 shows a plot of the Faraday rotation angle at 1152 nm against the magnetic field. It shows the clear saturation of the rotation angle at around 250 T, which is close to the 514.5 nm data. In this case, the experimental data show an agreement with the theoretical curve for an $S=\frac{1}{2}$ uniform Heisenberg antiferromagnetic chain at $T=0$ K. However, this might be inconsistent with the data of the temperature dependence of the magnetic susceptibility, which has the large deviation from the theoretical curve by Bonner and Fisher. This will be discussed in the next section. The Faraday rotation data agree well with the magnetization data up to 20 T measured by Ohta *et al.*[12] We put their data in Fig. 6 for comparison. These agreements show that at 1152 nm the Faraday rotation angle is almost linear to the magnetization because the photon energy is far from the $d\gamma$-$d\varepsilon$ transition energy. This saturation magnetization curve also shows that the $CuGeO_3$ can be considered as an $S=\frac{1}{2}$ one-dimensional Heisenberg antiferromagnet. The origin of the small deviation of the experimental data from the theoretical curve just below the saturation field is not clearly understood. This is not the rounding due to the effect of the finite temperature, because such a temperature effect can be neglected compared to the large Zeeman energy at 250 T.

Figure 7 shows the Faraday rotation data up to 150 T using the single turn coil technique. With this technique, we can investigate hysteric behavior, during the up and down sweeps of the magnetic field. We found that the magnetization deduced from the Faraday rotation shows a large hysteresis in the field range lower than 90 T at $T=6$ K. Above this field, the hysteresis disappeared as shown in Fig. 7. In order to investigate the relaxation rate of spins in the field-induced

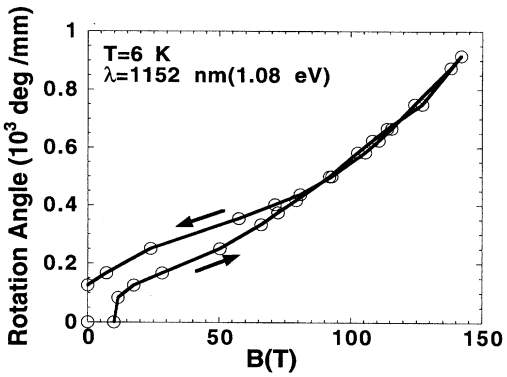

FIG. 7. Magnetization curve up to 150 T produced by the single turn coil technique. Solid line is the guide for eyes. There is a large hysteresis below 90 T and a finite magnetization remains at zero field. The field scanning speed is about 80 T/μs at zero field and 65 T/μs at 90 T.

magnetic phase, we measured the Faraday rotation with a slightly slower scanning rate of the magnetic field by decreasing the maximum field. Namely, the scanning speed in Fig. 7 was 65 T/μs at 90 T, but the measurement was done also with a speed of 23 T/μs (at 90 T) by setting the maximum field to 100 T. A similar hysteresis was observed also at this speed, and it disappeared at 90 T again. This result shows that the hysteresis is an inherent property which occurs only below 90 T, independent of the scan speed between 23 and 65 T/μs. The present observation strongly suggests that there is a large change in the relaxation speed across 90 T.

We found also that the hysteresis disappears when the temperature was increased above about 10 K. This result implies the system is considered to be in the uniform (U) phase in the range $T>10$ K and $H_c<H<150$ T.

Figure 8 shows the magnetization curves at lower fields around H_c, measured with different scanning speeds of the magnetic field. At a higher scan speed, there is a large hysteresis with a finite remnant magnetization as shown in (a). As shown in (b), the magnetization at a slower scan speed shows a smaller hysteresis without a remnant magnetization.

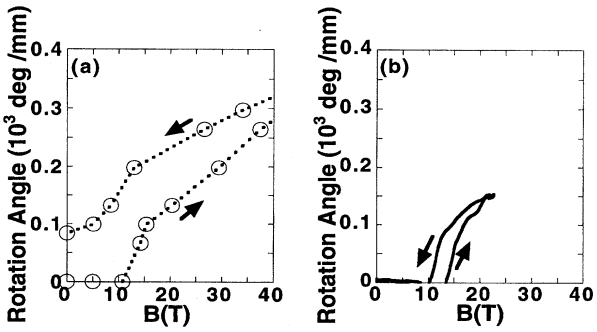

FIG. 8. Faraday rotation angle vs magnetic field at 7 K for different field scanning speeds. Dashed line is the guide for eyes. The field scanning speed at 12 T is about 60 T/μs for (a) and 10 T/μs for (b). The wavelength is 514.5 nm.

The hysteresis at H_c is still as large as 3.5 T. It should be noted that the observed hysteresis in the present measurement is much larger than those observed previously[6,12] in nondestructive fields whose scan speed is about 1000 times lower. The hysteresis in the latter case was several tens of mT at most.

Including the data shown in Fig. 6, where the field scan speed at H_c was 0.3 T/μs, the data in Figs. 6, 7, and 8 with different scan speeds indicate that the observed critical field H_c(obs) in the up trace increases as the scan speed becomes higher, but it never exceeds 15 T, while the H_c(obs) in the down trace shows a very large change as the scan speed is increased. In the down trace, even a remnant magnetization appears when the scan speed exceeds 60 T/μs. This asymmetric behavior across H_c is very different from the usual hysteresis observed in other first-order phase transitions such as the spin-flop transition in antiferromagnetic substances. The remnant magnetization might be caused by some irreversible process of the magnetization in the M phase.

In Fig. 8(b), the rotation angle is zero below the critical field H_c. Below H_c, the magnetization is zero because the system is in the nonmagnetic dimerized phase. In such a case, only the nonmagnetic part contributes to the Faraday rotation angle. The present result shows that the nonmagnetic part is negligibly small in $CuGeO_3$. This is also confirmed by the fact that the Faraday rotation is very small at room temperature, corresponding to the small magnetization.

IV. DISCUSSION

At the saturation field H_S, we can expect a relation

$$g\mu_B H_S = 4JS, \tag{3}$$

between the saturation field H_S and the exchange coupling J when the Hamiltonian of the system is expressed as Eq. (1). It is based on the assumption that the interchain coupling is comparatively smaller than the intrachain coupling, in other words, the value of J obtained from Eq. (3) is an effective exchange coupling constant between nearest-neighbor spins. The effect of the alternation can be neglected in the high field limit near the saturation field according to the calculation of Bonner *et al.*[11] as mentioned in Sec. III. From Figs. 5 and 6, $H_S = 253$ T is obtained. Using the g value of 2.15 along the a axis determined by Ohta *et al.*[12] we evaluate $J = 183$ K as the exchange coupling constant. It should be noted that this saturation field was measured at a finite temperature. Since the magnetization curves of an alternating system and a uniform system should be very similar around the saturation field as mentioned above, we estimated the effect of finite temperature by using the calculated magnetization curve for a uniform system at finite temperatures by Bonner and Fisher.[2] This correction is negligibly small in this case because the Zeeman energy at the saturation field is much larger than the thermal energy at around 6–7 K. The present value of the exchange coupling is determined by the most direct and clear method as compared to previous works.[1,3]

The magnetization curve we obtained shows an agreement with the theoretical curve for an $S = \frac{1}{2}$ uniform Heisenberg antiferromagnetic chain. However, the magnetic susceptibility data[1] show a deviation from the theoretical curve by Boner and Fisher. There are several arguments to explain the temperature dependence of the magnetic susceptibility, such as the temperature dependence of the exchange constant or the effect of the exchange coupling between next-nearest neighbors. Tonegawa and Motokawa[13] calculated the temperature dependence of the exchange coupling constant using the magnetic susceptibility data in Ref. 1 and the theoretical curve of Bonner and Fisher. The result shows that the exchange coupling constant varies more than 50% between room temperature and low temperatures. From this point of view, it is possible to explain the discrepancy between the magnetization and magnetic susceptibility data. However, it is necessary to obtain a clear view concerning the mechanism of this strong temperature dependence of the exchange constant to compare their idea with the present results. Recently, Riera and Dobry[14] calculated the magnetic susceptibility considering the second-neighbor interaction along the chain. Their results show a good agreement with experimental data when $J = 160$ K and the second-neighbor interaction of $0.36J$ are assumed. The saturation field of a system with a competing interaction from both the first and the second neighbors in one-dimensional antiferromagnets is determined mainly by the first-neighbor one. Tonegawa and Harada[15] calculated the saturation field of the one-dimensional isotropic spin-$\frac{1}{2}$ Heisenberg antiferromagnet with antiferromagnetic first- and second-neighbor interaction. According to their result, the correction of the saturation field by the second-neighbor interaction is very small even in the case of the significantly large second-neighbor interaction as assumed in the calculation of Riera and Dobry. However, the quantitative estimation of the second-neighbor contribution is difficult from the present experimental data alone, without a satisfactory theory of the magnetization curve for a spin-Peierls system with the first- and second-neighbor interactions.

An inelastic neutron scattering experiment is one of the powerful methods to estimate exchange constants. However, the formula which can be applied to magnetic excitations in a spin-Peierls system has not been obtained. In the case of an $S = \frac{1}{2}$ uniform Heisenberg antiferromagnetic chain, there is a formula by des Cloizeaux and Pearson,

$$E(q) = \frac{\pi J}{2} \sin(qc), \tag{4}$$

where q is the wave vector and c is the lattice spacing. In the case of the real spin-Peierls materials, the situation is more complicated because other factors such as the energy gap, interchain couplings, and anisotropy should be taken into account to evaluate J from the magnetic dispersion. Moreover, there is a fundamental question if the formula for a system without dimerization is applicable to a spin-Peierls system which has a completely different ground state from the Néel state. The discrepancy between the present value of J and the value in Ref. 3 can be reexamined if such a theoretical formula for a spin-Peierls system is obtained.

Next, we discuss the hysteresis in the magnetization process and the phase boundary between the M and U phases in sufficiently higher field above H_c. The existence of a large hysteresis in an isothermal magnetization curve is also re-

ported in organic spin-Peierls materials. Such a large hysteresis in the magnetization process of a spin-Peierls system can be explained as spins are coupled with the lattice and consequently the relaxation time may become longer compared to a system with simple antiferromagnetic long-range order. The large hysteresis shown in Fig. 7 disappears above 10 K. This suggests that the system is in the uniform phase above 10 K in the high magnetic fields between H_c and 150 T. We have to consider another possibility that the relaxation time becomes faster as the temperature is increased. The fact that the hysteresis shows almost no change in the temperatures between 5 and 9 K suggests that the former possibility is more plausible.

As is mentioned in Sec. III, the hysteresis disappears above a certain field of about 90 T when we applied the magnetic field of 150 T peak at $T=6$ K. We found that the hysteresis is still observed up to 90 T when we decreased the scan speed of the field. If the disappearance of the hysteresis is simply caused by the competition between the field scanning speed and the relaxation time and if the relaxation time is independent of magnetic-field intensity, it should have occurred at a lower magnetic field for slower scan speed. The present result suggests that the relaxation time changes when the field intensity is increased across 90 T in the magnetic phase. However, since there is no established theory of the magnetic properties of the spin-Peierls system in high magnetic fields well above H_c, the details of the microscopic mechanism of the observed large hysteresis still remains an open question.

V. SUMMARY

We have measured the Faraday rotation of $CuGeO_3$ in high magnetic fields up to 500 T in two photon energies of 2.41 and 1.08 eV. A distinct saturation of magnetization is observed at 253 T at both energies, and the exchange constant was evaluated as $J=183$ K. The contribution of the higher order terms in the Faraday rotation was observed at a photon energy of 2.41 eV, while it was negligible at 1.08 eV. At this energy, the magnetization curve derived from the Faraday rotation shows an agreement between the calculation for an $S=\frac{1}{2}$ uniform Heisenberg antiferromagnetic chain and a result of a previous measurement in lower fields. A large hysteresis was observed in the magnetization process below 10 K in the magnetization measurement up to 150 T by using the single turn coil technique. The hysteresis disappears above 90 T at 6 K but the five value relating the disappearance of the hysteresis does not change when the field scanning speed is decreased to 35%. This fact suggests that there is a large change in the relaxation time in the M phase in high magnetic field around 90 T.

ACKNOWLEDGMENTS

The authors express their thanks to Dr. H. Ohta (Kobe University, Japan), Professor I. Harada (Okayama University, Japan), and Professor H. Hori (J.A.I.S.T., Hokuriku, Japan) for valuable discussions and suggestions. This work was partly supported by the International Joint Research Grants of NEDO.

[1] M. Hase, I. Terasaki, and K. Uchinokura, Phys. Rev. Lett. **70**, 3651 (1993).
[2] J. C. Bonner and M. E. Fisher, Phys. Rev. **135**, A640 (1964).
[3] M. Nishi, O. Fujita, and J. Akimitsu, Phys. Rev. B **50**, 6508 (1994).
[4] J. des Cloizeaux and J. J. Pearson, Phys. Rev. **128**, 2131 (1962).
[5] R. B. Griffiths, Phys. Rev. **133**, A768 (1964).
[6] M. Hase, I. Terasaki, K. Uchinokura, M. Tokunaga, N. Miura, and H. Obara, Phys. Rev. B **48**, 9616 (1993).
[7] K. Nakao, F. Herlach, T. Goto, S. Takeyama, T. Sakakibara, and N. Miura, J. Phys. E. **18**, 1018 (1985).
[8] H. Nojiri, T. Takamasu, S. Todo, T. Haruyama, K. Uchida, H. A. Katori, T. Goto, and M. Miura, Physica B **201**, 579 (1994).
[9] N. Miura, H. Nojiri, T. Takamasu, T. Goto, K. Uchida, H. A. Katori, T. Haruyama, and S. Todo, in *Megagauss Magnetic Fields and Pulsed Power Applications*, Proceedings of the 6th International Conference of Megagauss Field Generation and Related Topics, Albuquerque, 1992, edited by M. Cowan and R. B. Spielman (Nova, Commack, NY, 1994), p. 125.
[10] I. Terasaki, R. Itti, N. Koshizuka, M. Hase, I. Tsukada, and K. Uchinokura (unpublished).
[11] J. C. Bonner, S. A. Friedberg, H. Kobayashi, D. L. Meier, and H. W. J. Blöte, Phys. Rev. B **27**, 248 (1983).
[12] H. Ohta, S. Imagawa, H. Ushiroyama, M. Motokawa, O. Fujita, and J. Akimitsu, J. Phys. Soc. Jpn. **63**, 2870 (1994).
[13] T. Tonegawa and M. Motokawa (unpublished).
[14] J. Reira and A. Dobry (unpublished).
[15] T. Tonegawa and I. Harada, J. Phys. Soc. Jpn. **56**, 2153 (1987).